Glucocorticoids promote Von Hippel Lindau degradation and Hif-1α stabilization

Andrea Vettori[a,1], David Greenald[b,c,d,1], Garrick K. Wilson[e,1], Margherita Peron[a], Nicola Facchinello[a], Eleanor Markham[b], Mathavan Sinnakaruppan[c,d], Laura C. Matthews[f], Jane A. McKeating[g,2,3], Francesco Argenton[a,2,3], and Fredericus J. M. van Eeden[b,2,3]

[a]Department of Biology, University of Padova, I-35121 Padova, Italy; [b]Bateson Centre, Department of Biomedical Science, University of Sheffield, Sheffield S10 2TN, United Kingdom; [c]Lee Kong Chian School of Medicine, Nanyang Technological University, 639798, Singapore; [d]Genome Institute of Singapore, 138672, Singapore; [e]Institute of Immunology and Immunotherapy, College of Medical and Dental Sciences, University of Birmingham, Birmingham B15 2TT, United Kingdom; [f]Leeds Institute of Cancer and Pathology, Faculty of Medicine and Health, University of Leeds, St James's University Hospital, Leeds LS9 7TF, United Kingdom; and [g]Nuffield Department of Medicine, University of Oxford, Oxford OX3 7BN, United Kingdom

Edited by Gregg L. Semenza, Johns Hopkins University School of Medicine, Baltimore, MD, and approved July 25, 2017 (received for review April 3, 2017)

Glucocorticoid (GC) and hypoxic transcriptional responses play a central role in tissue homeostasis and regulate the cellular response to stress and inflammation, highlighting the potential for cross-talk between these two signaling pathways. We present results from an unbiased in vivo chemical screen in zebrafish that identifies GCs as activators of hypoxia-inducible factors (HIFs) in the liver. GCs activated consensus hypoxia response element (HRE) reporters in a glucocorticoid receptor (GR)-dependent manner. Importantly, GCs activated HIF transcriptional responses in a zebrafish mutant line harboring a point mutation in the GR DNA-binding domain, suggesting a nontranscriptional route for GR to activate HIF signaling. We noted that GCs increase the transcription of several key regulators of glucose metabolism that contain HREs, suggesting a role for GC/HIF cross-talk in regulating glucose homeostasis. Importantly, we show that GCs stabilize HIF protein in intact human liver tissue and isolated hepatocytes. We find that GCs limit the expression of Von Hippel Lindau protein (pVHL), a negative regulator of HIF, and that treatment with the c-src inhibitor PP2 rescued this effect, suggesting a role for GCs in promoting c-src–mediated proteosomal degradation of pVHL. Our data support a model for GCs to stabilize HIF through activation of c-src and subsequent destabilization of pVHL.

hypoxia-inducible factor | glucocorticoid signaling | Von Hippel Lindau | metabolism | liver

Glucocorticoids (GCs) are steroid hormones secreted from the adrenal glands that regulate carbohydrate, lipid, and protein metabolism. GCs are widely used as anti-inflammatory agents for treating pathological conditions where hypoxia plays a role in disease progression such as rheumatoid arthritis and chronic obstructive pulmonary disease. GCs and hypoxia pathways have a close interplay in physiology and disease (1–3); however, recent studies report conflicting results on the cross-talk between GC action and hypoxia (4, 5). Hypoxia-inducible factors (HIFs) are oxygen-sensitive transcriptional complexes constituted by α- and β-subunits that activate diverse pathways regulating cellular glucose and lipid metabolism and proliferation (6, 7). Under normoxic conditions, the HIF-1α transcriptional subunit is recognized by prolyl hydroxylases and targeted for degradation via the Von Hippel Lindau (VHL)-mediated ubiquitin proteasome pathway; however, under hypoxic conditions HIF-1α is stabilized and translocates to the nucleus to exert its transcriptional activity. HIFs play a central role in many disease processes and provide a therapeutic target for treating pathological conditions including cancer, ischemia, stroke, inflammation, and chronic anemia (8–11). Screens to identify agents that stabilize HIFs have identified numerous agents, with the majority acting either via iron chelation or as 2-oxyglutarate analogs (12). In vitro HIF-reporter screening methods, although extremely valuable, do not provide physiological information and may overlook tissue-specific activators that require a physiological context.

To identify regulators of the HIF pathway, we developed several HIF-reporter zebrafish lines (13) and completed an unbiased chemical screen. GCs activated HIF-associated transcriptional responses most prominently in the liver. Importantly, we translate these observations to human tissue and show that GCs stabilize HIF in primary human hepatocytes and intact liver slices. Our data support a model where GCs act via a transcriptional independent mechanism by activating c-src to repress Von Hippel Lindau (pVHL) expression and stabilize HIF protein under normoxic conditions. Our study identifies a role for GCs to stabilize HIF and to regulate liver glucose metabolism.

Results

GCs Activate Hypoxic Signaling. Prolyl hydroxylase 3 (PHD3) transcription is regulated by HIFs, and we used our zebrafish *phd3:eGFP* HIF-reporter line to screen a chemical library (Dataset S1) for HIF activators. Dimethyloxaloylglycine (DMOG), a well-established activator of HIF signaling, was used as a positive control (14). Of the 41 initial hits, several GCs activated the reporter to comparable levels as DMOG (60 μM) (Fig. 1*A*). We confirmed that two GR agonists, betamethasone 17,21-dipropanoate (BME) and dexamethasone (DEX), activated the reporter (Fig. 1 *B* and *C*). We

Significance

An in vivo chemical screen in zebrafish identified glucocorticoids (GCs) as activators of hypoxia-inducible factor transcriptional responses in the liver. This cross-talk is conserved in human liver and requires glucocorticoid receptor signaling but not DNA binding. In human liver cells, GCs down-regulate Von Hippel Lindau expression at a posttranscriptional level most likely through c-src–mediated proteasomal degradation. Since the liver is an important regulator of blood glucose and hypoxia-inducible factors regulate gluconeogenesis/glycogen synthesis, cross-talk between these transcriptional regulators may be essential to control glucose metabolism in the liver. This identified, conserved, noncanonical pathway may have wider physiological significance in health and disease.

Author contributions: A.V., M.S., L.C.M., J.A.M., F.A., and F.J.M.v.E. designed research; A.V., D.G., G.K.W., M.P., N.F., E.M., and F.A. performed research; N.F., M.S., L.C.M., and F.J.M.v.E. contributed new reagents/analytic tools; A.V., D.G., G.K.W., M.P., E.M., J.A.M., F.A., and F.J.M.v.E. analyzed data; and A.V., D.G., G.K.W., L.C.M., J.A.M., F.A., and F.J.M.v.E. wrote the paper.

The authors declare no conflict of interest.

This article is a PNAS Direct Submission.

Freely available online through the PNAS open access option.

[1]A.V., D.G., and G.K.W. contributed equally to this work.

[2]J.A.M., F.A., and F.J.M.v.E. contributed equally to this work.

[3]To whom correspondence may be addressed. Email: jane.mckeating@ndm.ox.ac.uk, francesco.argenton@unipd.it, or f.j.vaneeden@sheffield.ac.uk.

This article contains supporting information online at www.pnas.org/lookup/suppl/doi:10.1073/pnas.1705338114/-/DCSupplemental.

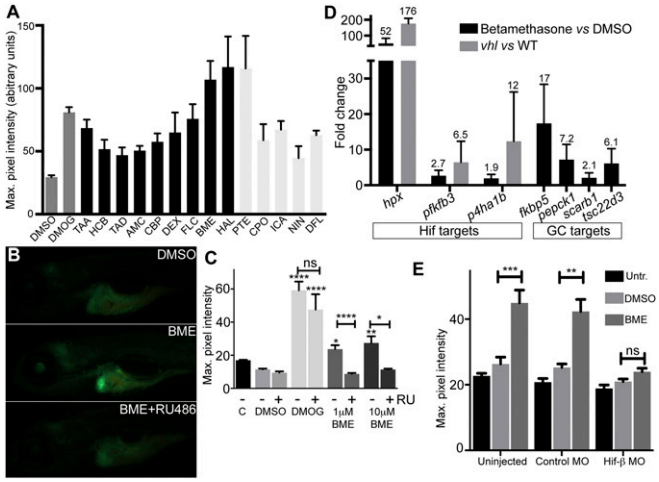

Fig. 1. Identification of glucocorticoids as HIF activators. (*A*) Retest of hits from the Spectrum screen for activators of the HIF response in phd3:eGFP zebrafish, where compounds showing an average GFP level of >44 are shown. Averaged maximum pixel intensity and SEM are shown for between five and nine embryos. Dark gray: controls; black: GC-like compounds; light gray: non-GC hits. AMC, amcinonide; BME, betamethasone; CBP, clobetasol propionate; CPO, ciclopirox olamine; DEX, dexamethasone; DFL, 8,2-dimethoxyflavone; FLC, fluocinonide; HAL, halcinonide; HCB, hydrocortisone butyrate; ICA, icariin; NIN, 7-nitroindazole; PTE, ptaeroxylin; TAA, triamcinolone acetonide; TAD, triamcinolone diacetate. (*B*) BME activates *phd3:eGFP* in an RU-486–dependent manner; representative images show the activation specific to the liver in BME-treated embryos and reduced GFP expression following BME+RU-486 cotreatment. (Magnification: 16×.) (*C*) Quantitation of *phd3:eGFP* response. DMSO was added to 1% vol/vol in all experiments except Control (C), DMOG to 60 μM, and RU-486 to 5 μM as indicated ($n \geq 9$). (*D*) BME induction of hypoxia-regulated genes and GC target genes, where values above bars indicate average fold change (FC) and triplicate samples of 20 embryos were used. For the hypoxia-induced genes, FC induction in *vhl* mutants vs. wild type is given as a comparison, where FC is calculated using ΔΔCT ± SEM. (*E*) HIF1β-MO abrogates BME activation of *phd3:eGFP*. Maximum pixel intensity in embryos as grouped by injection showing mean ± SEM ($n = 14$). Significance was calculated using Kruskal–Wallis one-way ANOVA followed by Dunn's multiple comparison test for treatments against DMSO (*$P < 0.05$; **$P < 0.01$; ***$P < 0.001$; ****$P < 0.0001$).

noted increased *phd3*-GFP expression mainly in the liver (Fig. 1*B*), suggesting that activation may be due to nonspecific stress as result of drug metabolism. To address this potential issue, reporter embryos were treated with GCs in the presence or absence of the GR antagonist RU-486 that reduced GFP intensity of BME-treated embryos (Fig. 1 *B* and *C*), while having minimal effect on DMOG-dependent activation (Fig. 1*C*), demonstrating that GC-augmented *phd3:eGFP* activity is GR-dependent.

To characterize the effects of BME on endogenous hypoxia-associated transcriptional responses, we quantified selected HIF-responsive genes (*pfkfb3*, *p4ha1b*, and *hpx*) and GR-responsive genes (*tsc22d3*, *scarb1*, *fkbp5*, and *pepck1*) (15–17) by qPCR. *phd3:eGFP* embryos [5 days postfertilization (dpf)] were treated with BME (10 μM) for 8 h before isolating RNA, the optimal time for *phd3* induction. (Fig. S1). BME induced the transcription of HIF-target genes to variable extents, albeit less than in a *vhl* mutant background, with *hpx* being the most responsive gene (Fig. 1*D*). To determine whether BME activation of *phd3:eGFP* reporter is HIF dependent, we silenced Hif-1β expression, an essential binding partner of both HIF-1α and HIF-2α (18). Hif-1β morphants were incubated with BME from 56 h postfertilization (hpf) until 72 hpf, and HIF-1β knockdown significantly reduced GFP intensity in the treated embryos compared with control morpholino (MO)-injected embryos (Fig. 1*E*), demonstrating that GC activation of *phd3:eGFP* is HIF-dependent.

To confirm that GCs directly activate HIF-transcriptional activity, we created a HIF reporter zebrafish expressing tandem copies of a hypoxia response element (HRE) driving eGFP expression, named *Tg(4xhre-tata:eGFP)*^{ia21}. Reporter activity is decreased in Hif-1β morphants and increased by expression of a dominant active form of *HIF-1α* mRNA or DMOG treatment, confirming that the transgene responds to modulators of the HIF-1–signaling pathway (Fig. 2 and Fig. S2). To examine the influence of GCs, the offspring obtained from a *Tg(4xhre-tata:eGFP)*^{ia21} carrier were exposed to increasing concentrations of DEX for 24 h. Treated embryos showed a dose-dependent activation of the *4xhre-tata* transgene, confirming that GCs activate HIF transcriptional responses under normoxic conditions (Fig. 3*A* and Fig. S3*A*). To independently assess whether GCs affect HIF-1 signaling and the glycolytic pathway, we analyzed the expression of three known hypoxia-dependent regulators of glucose metabolism in zebrafish (19) using whole-mount in situ hybridization (WISH); as expected, *pfkfb3*, *ldha*, and *glut1* were up-regulated after DEX treatment as a consequence of HIF-1 activation (Fig. S3*B*).

GC Activation of HIF Is Independent of GR DNA Binding. GCs regulate gene transcription through binding and activating cytoplasmic GR, through nuclear translocation, and through direct binding to GC response elements (GRE) (20). To analyze the mechanism

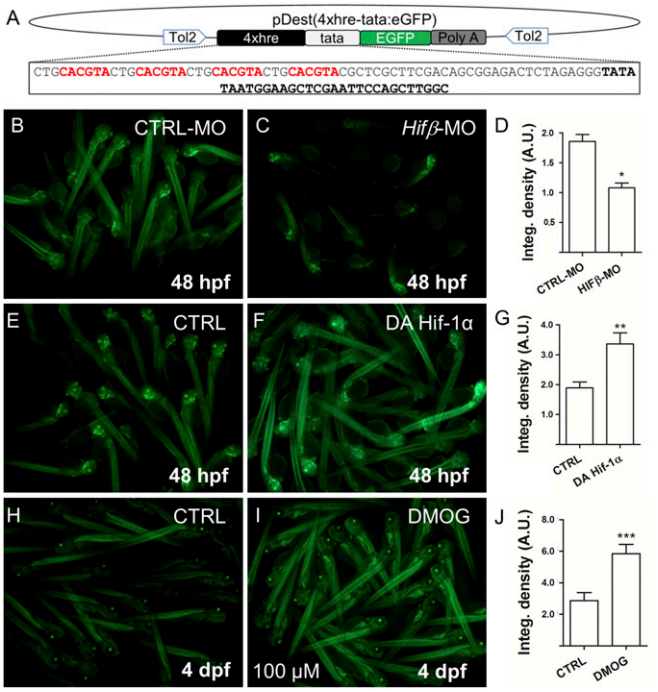

Fig. 2. Generation of *4xhre-tata* Hif-reporter lines. (*A*) Schematic representation of the Tol-2 vector used to generate the *Tg(4xhre-tata:eGFP)*^{ia21} line. The construct consists of a 98-bp fragment encoding four HREs (in red) from the murine lactate dehydrogenase followed by a TATA minimal promoter (in boldface), EGFP (in green), and the poly(A) signal. (*B–D*) Representative image of *Tg(4xhre-tata:eGFP)*^{ia21} embryos at 48 hpf injected with a control MO (*B*) or the HIFβ-MO MO (*C*). (Magnification: 5×.) Down-regulation of *Hifβ* significantly decreases transgene activity as reported by the integrated density analysis of fluorescence (*D*). (*E–G*) Hif-1α dominant active (DA) mRNAs injected in *Tg(4xhre-tata:eGFP)*^{ia21} embryos increase transgene expression (*F*) compared with control embryos (*E*). (Magnification: 5×.) (*H–J*) Treatment from 72 hpf to 96 hpf with 100 μM DMOG significantly increases 4xhre-tata transgene activity (*I*) with respect to the control embryos (*H*). (Magnification: 4×.) (*D*, *G*, and *J*) Average values of fluorescence integrated density calculated for treated embryos and controls. Values represent the mean ± SEM (***$P < 0.001$; **$P < 0.01$; *$P < 0.05$). A.U., arbitrary units.

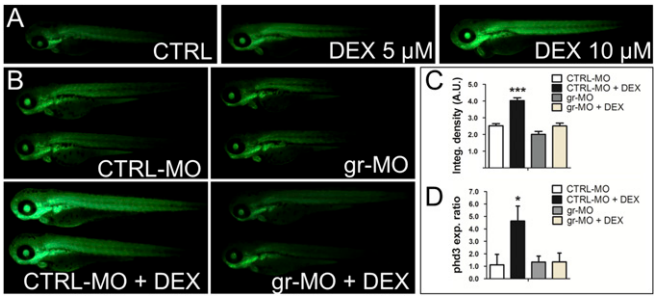

Fig. 3. Cross-talk between the HIF-1 and glucocorticoid-signaling pathways is mediated by the glucocorticoid receptor and HREs. (*A*) The 72-hpf *Tg(4xhre-tata:eGFP)*^{ia21} embryos were incubated with different concentrations of DEX. DEX activates the *4xhre-tata* transgene. (Magnification: 8×.) (*B*) Images of 72-hpf *Tg(4xhre-tata:eGFP)*^{ia21} larvae injected with a gr-MO and a CTRL-MO alone or combined with DEX (*Bottom*). DEX activation of *4xhre-tata* transgene expression is maintained in CTRL-MO–injected larvae and ablated in GR morphants. (Magnification: 8×.) (*C*) Histograms showing the average values (±SEM) of the fluorescence-integrated density in 72-hpf *Tg(4xhre-tata:eGFP)*^{ia21} embryos injected with gr-MO and CTRL-MO with or without DEX. A.U., Arbitrary units. (*D*) Fold changes (±SEM) in *phd3* gene expression in 72-hpf embryos injected with gr-MO and CTRL-MO with or without DEX (24 h) compared with non-treated/noninjected controls (set at 1). Target gene mRNA levels were normalized to β-actin. $*P < 0.05$; $***P < 0.001$.

underlying GC/HIF cross-talk, we assessed whether DEX-induced effects on HIF-reporter activity were dependent on GR and its DNA binding activity. Single-cell stage *Tg(4xhre-tata:eGFP)*^{ia21} embryos were microinjected with a splice-blocking MO against full-length GR (*gr*-MO) (21). Real-time PCR analysis of *fkbp5* showed significantly reduced expression to confirm gr-MO activity (Fig. S3*C*). Morphants and control *Tg(4xhre-tata:eGFP)*^{ia21} embryos (48 hpf) were incubated with or without DEX (10 μM) for 24 h, and reporter activity was measured. DEX increased *4xhre-tata* activity in controls but had minimal effect on the *gr* morphants (Fig. 3 *B* and *C*). Moreover, HIF activation was independently confirmed by measuring endogenous *phd3* mRNA expression in 72-hpf *gr* morphants and control embryos (Fig. 3*D*). Finally, GR dependency of HIF transcriptional activation was observed in a CRISPR-induced null mutant of the GR gene (Fig. S3*D*).

We also studied the zebrafish *gr*^{s357}mutant (22) that lacks DNA-binding function and abrogates GR transcriptional activity (Fig. 4*A*). Interestingly, DEX activated the *Tg(4xhre-tata:eGFP)*^{ia21} reporter in a *gr*^{s357} mutant background (Fig. 4*B*), suggesting that a non-transcriptional mechanism underlies GC activation of HIF signaling. To independently assess the role of the GR DNA-binding domain in GC/HIF cross-talk, offspring from two *gr*^{s357} homozygous carriers (72 hpf) were incubated with DEX or BME, and *phd3* mRNA levels were analyzed by WISH (Fig. 4 *C*–*E*). DEX and BME activated *phd3* transcription in both wild-type and *gr*^{s357} mutant embryos, confirming that HIF transcriptional activity was preserved.

GCs Activate HIF Signaling in Human Hepatocytes. To verify whether the GC/HIF cross-talk observed in zebrafish is relevant to humans, we focused our efforts on human liver-derived cells. Culturing hepatocyte-derived Huh-7 cells under low oxygen stabilized HIF-1α at comparable levels to prednisolone treatment (Fig. 5 *A* and *B*). To assess transcriptional responses, Huh-7 cells were transfected with a *hre-luciferase* (*hre-luc*) reporter and treated with prednisolone and dexamethasone that activated the reporter (Fig. 5*C*). Furthermore, prednisolone induced mRNA levels of three endogenous HIF target genes (*VEGF*, *PDK*, and *GLUT1*) to a similar degree as low-oxygen treatment, thus paralleling the in vivo results observed in zebrafish embryos (Fig. 5*D*). Furthermore, GC activation of HRE activity was sensitive to the GR antagonist RU-486 (Fig. 5*D*), demonstrating GR dependency. Next we screened a panel of hypoxia-regulated target genes in Huh-7 cells and found that 29/38 HIF target genes were induced by prednisolone, whereas only 3 of 38 were induced by cortisone (Dataset S2).

To confirm that the response is not simply a result of using immortalized Huh-7 cells, we showed that prednisolone activated the HRE reporter in primary human hepatocytes (Fig. 5*E*). To ascertain whether GCs increase HIF expression and associated transcriptional activity in an authentic liver microenvironment, we treated human liver slices with prednisolone or culture under low oxygen (3%) for 16 h and imaged nuclear HIF-1α (Fig. 6*A*) and quantified HIF target gene mRNA levels (Fig. 6 *B* and *C*). Both prednisolone and low-oxygen treatments stabilized HIF-1α (Fig. 6*A*) and increased HIF target gene expression (Fig. 6 *B* and *C*). Together, these data demonstrate that, as in the zebrafish, GCs can activate HIF signaling in the human liver.

To determine how GCs activate HIF signaling, we investigated the effect of GCs on pVHL expression, a crucial negative regulator of HIFα protein. We showed that GCs reduce pVHL expression in Huh-7 cells (Fig. 6*D*). This is unlikely to be mediated by a transcriptional mechanism since VHL mRNA levels were not affected (Fig. S4*A*). pVHL is degraded by the proteasome (Fig. 6*D*) following posttranslational modification by kinases such as c-src and CKII (24). Indeed, we found that inhibiting c-src activity with PP2 (25) rescued the inhibitory effects of GC on VHL expression (Fig. 6*E*), blocked HIF-1α induction (Fig. 6*F*), and normalized HIF

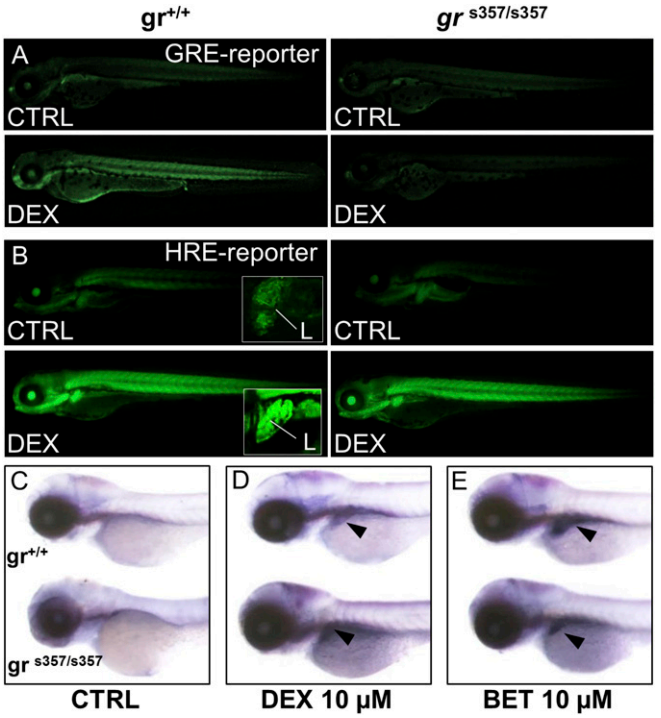

Fig. 4. Glucocorticoid induction of HIF-1 activity is independent of glucocorticoid receptor DNA binding. (*A*) Treatment with 10 μM DEX for 24 h activates the wild-type *Tg(9xGCRE-HSV.Ul23:eGFP)*^{ia20} (23) glucocorticoid reporter (GRE-reporter) line, while in *gr*^{s357} mutant background (*Right*) DEX is unable to activate GRE reporter. (Magnification: 14.5×.) (*B*) Images of wild-type and *gr*^{s357} embryos in the *Tg(4xhre-tata:eGFP)*^{ia21} background (HRE-reporter), treated for 24 h with DEX 10 μM. DEX activates the 4xhre-tata transgene in both wild-type and *gr*^{s357} mutant larvae and induces a significant and generalized increase of fluorescence that is particularly evident in the liver (L in *Insets*). (Magnification: 14.5×; *Insets*, 72.5×.) (*C*–*E*) In situ hybridization of *phd3* mRNA antisense probe in wild-type and *gr*^{s357} mutants at 80 hpf. (Magnification: 17.5×.) DEX (*D*) or BME (*E*) activated phd3 gene expression in the liver (arrowheads).

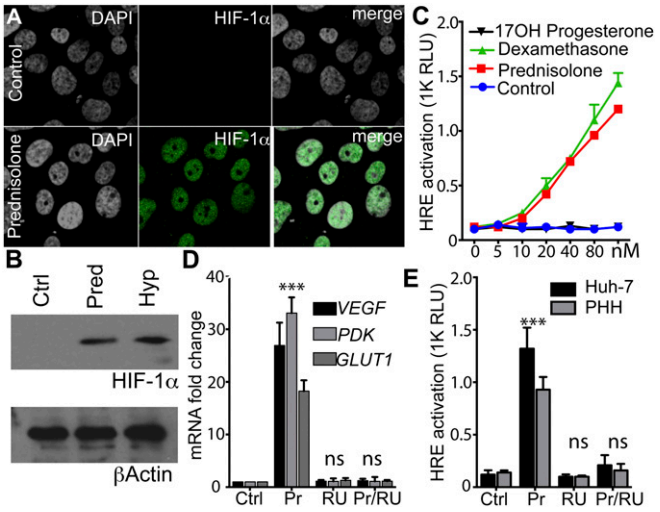

Fig. 5. Glucocorticoids stabilize HIF in human cell lines. (*A*) Mock or prednisolone-treated (100 nM) Huh-7 cells were stained for HIF-1α expression (green) and counterstained with DAPI (gray); images show nuclear localization of HIF-1α. (Magnification: 260×.) (*B*) HIF-1α expression in hypoxic (3% O_2) and prednisolone (Pred)-treated Huh-7 cells. (*C*) Huh-7 cells were transfected with a HRE luciferase reporter and 24 h later treated with increasing doses of various steroids (100 nM) for16 h. GC agonists activated the HRE reporter while 17OH did not. (*D*) Huh-7 cells treated with Pred/RU-486 (100 nM) for 24 h, lysed, and RNA-purified to quantify HIF transcriptional targets. Data represents fold change over control sample (Dataset S2). (*E*) Huh-7 cells and primary human hepatocytes (PHH) were transfected with a HRE luciferase reporter and 24 h later treated with Pred (100 nM) and/or RU-486 (100 nM) for 16 h, and HRE luciferase activity was measured. ***$P < 0.001$; ns, not significant (ANOVA). Data are represented as mean ± SD.

target gene expression (Fig. S4*B*), suggesting a mechanism for GCs to stabilize HIFs via degrading VHL.

Discussion

The Spectrum Collection (Microsource Discovery Systems) includes compounds that modulate a wide variety of pathways; however, only GCs showed a consistent and robust HIF activation. It is surprising that GCs were not previously identified as HIF modifiers in cell-based chemical screens. We can only speculate what the apparent liver specificity of the GC effect may have contributed. Thus, in vivo chemical screens, providing a variety of cell types in a physiological context, are a useful expansion compared with more classical screening approaches, even with "well-trodden" pathways like HIF.

We confirmed that GCs promote HRE-dependent HIF transcriptional activity in fish and human liver cells. Surprisingly, fish expressing a GR mutant lacking a functional DNA-binding domain (DBD) still activated the *phd3* promoter and 4xhre reporter models after treatment with DEX. However, complete knockdown of GR and a newly generated truncated GR mutant abrogated the ability of DEX to stabilize HIF. The GR is essential for survival as demonstrated by the report that 90% of GR KO mice die soon after birth (26) and only 10% of GR KO zebrafish survive, with a reduced fitness. Of note, both mouse and zebrafish homozygous mutants of the GR-DBD survive with minor defects (22, 27), suggesting essential roles for GRE-independent GR activities, as exemplified by our study.

Since GCs are reported to activate c-src kinase (28, 29), which is known to phosphorylate and target pVHL for proteosomal degradation (24), we hypothesized a role for GCs in stabilizing HIF via c-src degradation of VHL. Consistent with our results, RU-486 inhibited such nongenomic effects of GR (30). Our in vitro studies confirm that GCs destabilize VHL protein expression, and this was rescued by cotreating cells with the c-src inhibitor PP2 (Fig. 6*E*). As VHL is a negative regulator of HIF, this results in HIF expression under normoxic conditions.

Although we see activation of *phd3* and 4xhre promoters and other hypoxia response genes by GCs, GCs do not fully replicate a hypoxic response. We find increased expression of many HIF target genes (Dataset S2), but some exceptions were noted such as Enolase1 and Carbonic anhydrase 9, which were down-regulated by prednisolone. A direct interaction between ligand-activated GR and HIF proteins cannot be excluded, as Kodama et al. (5) have suggested that GR binds the HIF dimer. However, a simpler explanation is that, in addition to stabilizing HIF protein, GR binds a subset of promoters to regulate transcription. A complex interplay is suggested by other reports: for example, while HIF up-regulates VEGF expression and promotes angiogenesis, GCs are generally angiostatic (31) and negatively regulate VEGF expression (32–34). Similarly, during high altitude sickness, GC and HIF may have apparently opposing effects (35, 36). Therefore, we propose that the interplay that we have identified is likely to be tissue- and possibly context-specific.

We found that GC agonists increased mRNA levels of the classical HIF target *erythropoietin* both in cell culture (Dataset S2) and in zebrafish embryos and adult zebrafish livers (Fig. S5). Our data are consistent with reports showing a synergistic effect of GCs and HIFs in hematopoiesis (37, 38), and it will be interesting to investigate whether this cooperativity is GR-DBD–dependent. GCs received their name because they promote blood glucose levels as well as gluconeogenesis and glycogen storage in the liver and provide an acute response to stress (39). HIF signaling has a profound impact on cellular metabolism and induces gluconeogenesis and glycogen storage (40, 41). We suggest that GCs modulation of VHL and HIF may contribute to their ability to modulate blood glucose and glycogen storage. In addition, HIF has been shown to impact lipid metabolism in the liver, where its (in)appropriate activation reduces beta oxidation and increases lipid storage capacity leading to steatosis (42, 43). It is worth noting that long-term treatment with GCs was reported to increase

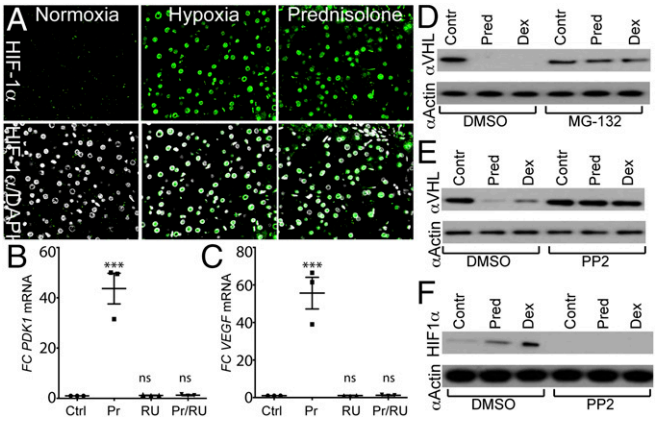

Fig. 6. Glucocorticoids stabilize HIF in human liver slices. (*A*) HIF-1α expression in human liver slices treated with prednisolone or cultured under low oxygen (3%) for 24 h and counterstained with DAPI. Both prednisolone and hypoxic treatments induce nuclear HIF-1α expression. Images are representative of five donor livers. (Magnification: 55×.) (*B* and *C*) HIF target gene *PDK1* and *VEGF* mRNA levels in human liver slices from three donors treated with Pred/RU-486 for 24 h. (*D*) VHL expression in Huh-7 cells treated with prednisolone (Pred) or dexamethasone (Dex) in presence or absence of proteasome inhibitor MG-132 at 10 μM. (*E* and *F*) Huh-7 cells treated with prednisolone (Pred) or dexamethasone (Dex) in presence or absence of Src inhibitor PP2 at 5 μM and probed for VHL (*E*) or HIF-1α (*F*). All samples were stained for actin as a loading control. ***$P < 0.001$; ns, not significant (ANOVA). Data are represented as mean ± SD.

steatosis (44). Activation of the HIF pathway via cross-talk with the GR may explain how GC excess regulates hepatic fat metabolism and the steatotic phenotype. Our experiments show that GCs predominantly stabilize HIF in the liver and may activate only a subset of HIF targets, which could be addressed by studying tissue-specific knockout models. Based on the elegant experiments of Rankin et al. (43), we would predict that liver-specific deletion of HIF-2a should protect mice from GC-induced steatosis and may reduce the effect of GCs on blood glucose levels.

It is becoming clear that HIF signaling is regulated not only by low oxygen, but also by several other inflammatory mediators (45–47). Our data support GC as a further key modulator of HIF signaling to add to this growing list. It is interesting to note that many common GC and HIF gene targets are implicated in regulating hepatic metabolism. This is potentially important, as GCs are secreted in a rhythmic circadian fashion, where circulating GC levels reach a maximum to coincide with the onset of the active phase—morning in humans, evening in mice. Since metabolic processes in the liver are coupled to the circadian clock, our data provide an additional level of control, where GC activation of the HIF pathway helps to ensure that the changing metabolic demands throughout the day are met. Our data suggest a role for GC-driven circadian components in other aspects of HIF signaling.

Material and Methods

Zebrafish Strains. *vhl* mutant and *Tg(phd3:eGFP)*$^{i144/i144}$ (13) fish were maintained in a mixed Tupfel long fin/London wild-type (TL/LWT) background. The *Tg(9xGCRE-HSV.Ul23:eGFP)*^{ia20} line is a GC pathway reporter (23). The zebrafish GR mutant line *gr*^{s357} was incrossed to create homozygotes (22). To obtain wild-type embryos, LWTs were incrossed. To obtain homozygous *vhl* mutants, *vhl*$^{hu2117/+}$; *phd3:eGFP*$^{i144/i144}$ fish were incrossed. Embryos were incubated at 28 °C in E3 (5 mM NaCl, 0.17 mM KCl, 0.33 mM CaCl2, 0.33 mM MgCl2, pH 7.2) containing methylene blue (Sigma-Aldrich) at 0.0001%. The generation of *Tg(4xhre-tata:eGFP)*^{ia21} and *Tg(4xhre-tata:mCherry, cmlc2:eGFP)*^{ia22} reporters and GR CRISPR mutation is described in *SI Text*.

Drug Treatment of Embryos. The Spectrum Collection (Microsource Discovery Systems) of 2,000 compounds was used; tested compounds and detailed methods can be found in *SI Text* and Dataset S1.

Hypoxic Target Gene Activation in Zebrafish. Three biological replicates of 10 *phd3:EGFP*$^{i144/i144}$ embryos were treated for 8, 12, 24, 36, and 48 h starting from 72 hpf. Embryos were treated with 10 μM betamethasone 17,21 dipropanoate and 60 μM DMOG in 1% DMSO, with untreated and 1% DMSO controls. The *vhl*$^{hu2117/hu2117}$; *phd3:EGFP*$^{i144/i144}$mutants were used as positive controls. Biological replicates of 48-hpf *Tg(4xhre-tata:eGFP)*^{ia21} embryos were incubated with or without 10 μM DEX and/or 3.8 μM 17-AAG (Sigma) for 24 h. RNA was isolated using TRIzol and quantified using the Nanodrop ND-1000 spectrophotometer. cDNA was reverse-transcribed from 0.5 μg RNA using the SuperScript III First-Strand Synthesis System (Invitrogen). For the temporal *phd3* expression profile, qPCR was performed with optimized primers, using the iCycler iQ system (Bio-Rad). Cycling conditions were the following: 95 °C – 3 min, [95 °C – 15 s, 60 °C – 30 s] × 40 cycles, 55–95 °C in 0.5-°C increments 30 s, with β-actin2 as internal control. Primers: see Dataset S3. For hypoxia/glucocorticoid target gene detection, qPCR was carried out using the Applied Biosystems SDS Software v2.4.1 in conjunction with the 7900HT Fast Real-Time qPCR System. The cycling conditions were the following: 50 °C – 2 min, 95 °C – 10 min, [95 °C – 15 s, 60 °C – 1 min] × 40 cycles. Primers: see Dataset S3. Cycle threshold (Ct) values were calculated automatically using the software, with ROX reference dye as the passive reference. Fold change was calculated using the ΔΔCT method.

MO and mRNA Injections. The translation-blocking MO HIFβ-MO (GGATTAGCTGATGTCATGTCCGACA) was used as reported (18) while a splice-site targeting MO (gr-MO) was used to silence GR (21). A standard control MO (CTRL-MO; Genetools) was used as a negative control. The MO stock solution (8 mg/mL) was diluted in Danieau's solution, and ∼2 nL was injected per embryo as previously described (48). Dominant-active *hif-1αa* and *hif-1αb* (kindly provided by P. Elks, University of Sheffield, Sheffield, UK) were synthesized (mMessageMachine; Ambion, Invitrogen) and injected as described in ref. 49.

Image Analysis in *Tg(4xhre-tata:eGFP)*^{ia21} Embryos. For analysis of *Tg(4xhre-tata:eGFP)*^{ia21} embryos, fluorescence was collected using a Leica M165FC dissecting microscope and a Nikon C2 H600L confocal microscope. *N*-phenylthiourea–treated larvae were anesthetized with tricaine and embedded in 1% low-melting agarose on a glass slide. Images were analyzed with Nikon software. For fluorescence quantification of transgenic embryos, a Leica M165FC microscope and DC500 digital camera were used. All images were acquired using identical parameters, and fluorescence-integrated density was calculated using ImageJ.

Cell Culture, Antibodies, and Treatments. Huh-7 and HEK293 cells were maintained in Dulbecco's modified Eagle's medium supplemented with 10% FBS, 1% L-glutamine, and 50 units/mL penicillin/streptomycin (Life Technologies). Primary human hepatocytes were isolated as described (50) and maintained in Williams E Medium (Sigma) supplemented with 10% FBS, 5 mM Hepes/insulin/L-glutamine (Life Technologies). Cells were grown in a humidified incubator at 37 °C, 5% CO_2, and 20% O_2 (normoxia). For hypoxic conditions, cells were grown at 37 °C in a humidified sealed Galaxy 48R incubator (New Brunswick) at 37 °C, 5% CO_2, 92% N_2, and 3% O_2 (hypoxia). The following antibodies used: anti-mouse HIF-1α (Novus Biologicals), anti-VHL (Cell Signaling #2738), Alexa Fluor goat anti-mouse 488 (Molecular Probes), anti–β-actin antibody (Sigma Aldrich), anti-mouse and anti-rabbit HRP-conjugated secondary antibody (GE Healthcare). Prednisolone, dexamethasone, cortisone, RU-486 17OH progesterone, and MG-132 are from Sigma Aldrich. Src inhibitor PP2 was purchased from Merk Millipore.

Ex Vivo Liver Slices. Liver tissue samples were collected with local National Health Service research ethics committee approval (Walsall LREC 04/Q2708/40) and with written informed consent. Donor liver tissue surplus to transplantation requirements were collected from the Queen Elizabeth Hospital. Cores were cut from the tissue immediately upon receipt using a Krumdieck Tissue Slicer (Alabama R&D) (51). Briefly, the core was placed into the slicer assembly under aseptic conditions, and 240-μm sections were collected and immediately transferred into Williams E media/1% L-glutamine/0.5 μM insulin. An albumin ELISA (Bethyl Laboratories) was used to monitor the viability of the slices. Samples from five donors were serum-starved followed by incubation under hypoxia (3% O_2) or normoxia (20% O_2) for 24 h. Liver slices were treated with prednisolone (100 nM) for 24 h before fixing for detection of HIF-1α by confocal microscopy.

Confocal Microscopy on Cells. Cells were grown on 13-mm borosilicate glass coverslips at a density of 4×10^4/well for 24 h and serum-starved for 5 h before treating with prednisolone (100 nM). Cells or liver slices were fixed in 3% paraformaldehyde for 25 min at room temperature (RT) and permeabilized with 0.01% TX-100/PBS for 10 min. Cells were incubated with anti–HIF-1α for 1 h at RT, unbound antibody was removed by washing, and bound antibody was detected with Alexa-488 secondary antibody. Nuclei were counterstained with 4′,6-diamidino-2-phenylindole, dihydrochlorine (DAPI; Life Technologies). Cells were imaged using a Zeiss Meta Head confocal microscope with a 63× water immersion objective.

HRE Reporter Assay. Cells were transfected with the HRE reporter (a plasmid containing four tandem HRE copies kindly provided by M. Ashcroft, Cambridge University, Cambridge, UK) using Fugene 6 transfection reagent (Promega) per the manufacturer's guidelines. After 24 h, cells were serum-starved for 5 h before treating with GC or RU-486, (100 nM) for a further 24 h. Cells were lysed, and reporter activity was quantified using a firefly luciferase assay system (Promega) in a luminometer (Berthold Lumat LB 9507).

Western Blotting. Cells were harvested in lysis buffer (PBS/1% Triton-X100/0.1% Na deoxycholate/0.1% SDS) containing protease and phosphatase inhibitors (Roche). Lysates were clarified by centrifugation, and protein concentration was determined using a Bradford Protein Assay Reagent (Pierce). Protein lysates (20 μg) were added to sample running buffer (30% glycerol/6% SDS/0.02% bromophenol blue/10% 2-β-mercaptoethanol/0.2 M Tris·HCl; pH 6.8) and separated by SDS/PAGE. Separated proteins were transferred to PVDF membranes and incubated with primary antibodies before detection with HRP-conjugated secondary antibody and enhanced chemiluminescence (Geneflow) using a PXi imaging system (Syngene).

ACKNOWLEDGMENTS. We thank the University of Sheffield and University of Padova aquaria teams for excellent care of zebrafish; J. Tomlinson and A. Clarke for critically reading the manuscript; M. Ashcroft (Cambridge University) for the HRE luciferase construct; P. Elks (University of Sheffield) for DA-Hif1 constructs; H. Baier (Max Planck Institute) for *gr*^{s357} mutants; and L. Dalla

Valle and E. Colletti for help in Padova. Work in the J.A.M. laboratory is funded by the National Institute for Health Research Birmingham Liver Biomedical Research Unit; Medical Research Council Programme Grant G1100247, European Union (EU) FP7 PathCo HEALTH Grant 597F3-2012–305578 and EU Horizon 2020 Hep-CAR Grant 667273. Work in the F.J.M.v.E. laboratory was supported by European Commission FP7 Grant HEALTH-F4-2010-242048 and Biology and Biotechnology Research Council Grant BB/M02332X/1 and an A*Star studentship (to D.G.). Work in the F.A. laboratory is funded by EU Project Grant ZF-HEALTH CT-2010-242048 and by Associazione Italiana per la Ricerca sul Cancro Project IG 10274. L.C.M. is supported by a University of Leeds Academic Fellowship. A.V. is supported by the Italian National Institute of Health Grant GR-2011-02346749.

1. Wright A, Brearey S, Imray C (2008) High hopes at high altitudes: Pharmacotherapy for acute mountain sickness and high-altitude cerebral and pulmonary oedema. *Expert Opin Pharmacother* 9:119–127.
2. Dardzinski BJ, et al. (2000) Increased plasma beta-hydroxybutyrate, preserved cerebral energy metabolism, and amelioration of brain damage during neonatal hypoxia ischemia with dexamethasone pretreatment. *Pediatr Res* 48:248–255.
3. Tokudome S, et al. (2009) Glucocorticoid protects rodent hearts from ischemia/reperfusion injury by activating lipocalin-type prostaglandin D synthase-derived PGD2 biosynthesis. *J Clin Invest* 119:1477–1488.
4. Wagner AE, Huck G, Stiehl DP, Jelkmann W, Hellwig-Bürgel T (2008) Dexamethasone impairs hypoxia-inducible factor-1 function. *Biochem Biophys Res Commun* 372:336–340.
5. Kodama T, et al. (2003) Role of the glucocorticoid receptor for regulation of hypoxia-dependent gene expression. *J Biol Chem* 278:33384–33391.
6. Semenza GL (2011) Regulation of metabolism by hypoxia-inducible factor 1. *Cold Spring Harb Symp Quant Biol* 76:347–353.
7. Kaelin WG, Jr (2011) Cancer and altered metabolism: Potential importance of hypoxia-inducible factor and 2-oxoglutarate-dependent dioxygenases. *Cold Spring Harb Symp Quant Biol* 76:335–345.
8. Bernhardt WM, et al. (2006) Preconditional activation of hypoxia-inducible factors ameliorates ischemic acute renal failure. *J Am Soc Nephrol* 17:1970–1978.
9. Shen X, et al. (2009) Prolyl hydroxylase inhibitors increase neoangiogenesis and callus formation following femur fracture in mice. *J Orthop Res* 27:1298–1305.
10. Shi T, et al. (2010) High-throughput screening identifies CHMP4A associated with hypoxia-inducible factor 1. *Life Sci* 87:604–608.
11. Wan C, et al. (2008) Activation of the hypoxia-inducible factor-1alpha pathway accelerates bone regeneration. *Proc Natl Acad Sci USA* 105:686–691.
12. Scholz CC, Taylor CT (2013) Targeting the HIF pathway in inflammation and immunity. *Curr Opin Pharmacol* 13:646–653.
13. Santhakumar K, et al. (2012) A zebrafish model to study and therapeutically manipulate hypoxia signaling in tumorigenesis. *Cancer Res* 72:4017–4027.
14. Jaakkola P, et al. (2001) Targeting of HIF-alpha to the von Hippel-Lindau ubiquitylation complex by O_2-regulated prolyl hydroxylation. *Science* 292:468–472.
15. van Rooijen E, et al. (2009) Zebrafish mutants in the von Hippel-Lindau tumor suppressor display a hypoxic response and recapitulate key aspects of Chuvash polycythemia. *Blood* 113:6449–6460.
16. Ciesek S, et al. (2010) Glucocorticosteroids increase cell entry by hepatitis C virus. *Gastroenterology* 138:1875–1884.
17. Schaaf MJ, Chatzopoulou A, Spaink HP (2009) The zebrafish as a model system for glucocorticoid receptor research. *Comp Biochem Physiol A Mol Integr Physiol* 153:75–82.
18. Prasch AL, Tanguay RL, Mehta V, Heideman W, Peterson RE (2006) Identification of zebrafish ARNT1 homologs: 2,3,7,8-tetrachlorodibenzo-p-dioxin toxicity in the developing zebrafish requires ARNT1. *Mol Pharmacol* 69:776–787.
19. Greenald D, et al. (2015) Genome-wide mapping of Hif-1α binding sites in zebrafish. *BMC Genomics* 16:923.
20. Becker PB, Gloss B, Schmid W, Strähle U, Schütz G (1986) In vivo protein-DNA interactions in a glucocorticoid response element require the presence of the hormone. *Nature* 324:686–688.
21. Pikulkaew S, et al. (2011) The knockdown of maternal glucocorticoid receptor mRNA alters embryo development in zebrafish. *Dev Dyn* 240:874–889.
22. Ziv L, et al. (2013) An affective disorder in zebrafish with mutation of the glucocorticoid receptor. *Mol Psychiatry* 18:681–691.
23. Benato F, et al. (2014) A living biosensor model to dynamically trace glucocorticoid transcriptional activity during development and adult life in zebrafish. *Mol Cell Endocrinol* 392:60–72.
24. Chou MT, Anthony J, Bjorge JD, Fujita DJ (2010) The von Hippel-Lindau tumor suppressor protein is destabilized by Src: Implications for tumor angiogenesis and progression. *Genes Cancer* 1:225–238.
25. Hanke JH, et al. (1996) Discovery of a novel, potent, and Src family-selective tyrosine kinase inhibitor. Study of Lck- and FynT-dependent T cell activation. *J Biol Chem* 271:695–701.
26. Cole TJ, et al. (2001) GRKO mice express an aberrant dexamethasone-binding glucocorticoid receptor, but are profoundly glucocorticoid resistant. *Mol Cell Endocrinol* 173:193–202.
27. Reichardt HM, et al. (1998) DNA binding of the glucocorticoid receptor is not essential for survival. *Cell* 93:531–541.
28. Kayahara M, et al. (2008) MNAR functionally interacts with both NH2- and COOH-terminal GR domains to modulate transactivation. *Am J Physiol Endocrinol Metab* 295:E1047–E1055.
29. Matthews L, et al. (2008) Caveolin mediates rapid glucocorticoid effects and couples glucocorticoid action to the antiproliferative program. *Mol Endocrinol* 22:1320–1330.
30. Croxtall JD, Choudhury Q, Flower RJ (2000) Glucocorticoids act within minutes to inhibit recruitment of signalling factors to activated EGF receptors through a receptor-dependent, transcription-independent mechanism. *Br J Pharmacol* 130:289–298.
31. Shikatani EA, et al. (2012) Inhibition of proliferation, migration and proteolysis contribute to corticosterone-mediated inhibition of angiogenesis. *PLoS One* 7:e46625.
32. Hegeman MA, et al. (2013) Dexamethasone attenuates VEGF expression and inflammation but not barrier dysfunction in a murine model of ventilator-induced lung injury. *PLoS One* 8:e57374.
33. Greenberger S, Boscolo E, Adini I, Mulliken JB, Bischoff J (2010) Corticosteroid suppression of VEGF-A in infantile hemangioma-derived stem cells. *N Engl J Med* 362:1005–1013.
34. Shim SH, Hah JH, Hwang SY, Heo DS, Sung MW (2010) Dexamethasone treatment inhibits VEGF production via suppression of STAT3 in a head and neck cancer cell line. *Oncol Rep* 23:1139–1143.
35. Bigham AW, Lee FS (2014) Human high-altitude adaptation: Forward genetics meets the HIF pathway. *Genes Dev* 28:2189–2204.
36. Prabhakar NR, Semenza GL (2012) Adaptive and maladaptive cardiorespiratory responses to continuous and intermittent hypoxia mediated by hypoxia-inducible factors 1 and 2. *Physiol Rev* 92:967–1003.
37. Bauer A, et al. (1999) The glucocorticoid receptor is required for stress erythropoiesis. *Genes Dev* 13:2996–3002.
38. Flygare J, Rayon Estrada V, Shin C, Gupta S, Lodish HF (2011) HIF1alpha synergizes with glucocorticoids to promote BFU-E progenitor self-renewal. *Blood* 117:3435–3444.
39. Kuo T, McQueen A, Chen TC, Wang JC (2015) Regulation of glucose homeostasis by glucocorticoids. *Adv Exp Med Biol* 872:99–126.
40. Park SK, Haase VH, Johnson RS (2007) von Hippel Lindau tumor suppressor regulates hepatic glucose metabolism by controlling expression of glucose transporter 2 and glucose 6-phosphatase. *Int J Oncol* 30:341–348.
41. Choi JH, et al. (2005) Molecular mechanism of hypoxia-mediated hepatic gluconeogenesis by transcriptional regulation. *FEBS Lett* 579:2795–2801.
42. Liu Y, et al. (2014) HIF-1α and HIF-2α are critically involved in hypoxia-induced lipid accumulation in hepatocytes through reducing PGC-1α-mediated fatty acid β-oxidation. *Toxicol Lett* 226:117–123.
43. Rankin EB, et al. (2009) Hypoxia-inducible factor 2 regulates hepatic lipid metabolism. *Mol Cell Biol* 29:4527–4538.
44. Patel R, Williams-Dautovich J, Cummins CL (2014) Minireview: New molecular mediators of glucocorticoid receptor activity in metabolic tissues. *Mol Endocrinol* 28:999–1011.
45. Bullen JW, et al. (2016) Protein kinase A-dependent phosphorylation stimulates the transcriptional activity of hypoxia-inducible factor 1. *Sci Signal* 9:ra56.
46. D'Ignazio L, Bandarra D, Rocha S (2016) NF-κB and HIF crosstalk in immune responses. *FEBS J* 283:413–424.
47. Peyssonnaux C, et al. (2005) HIF-1alpha expression regulates the bactericidal capacity of phagocytes. *J Clin Invest* 115:1806–1815.
48. Vettori A, et al. (2011) Developmental defects and neuromuscular alterations due to mitofusin 2 gene (MFN2) silencing in zebrafish: A new model for Charcot-Marie-Tooth type 2A neuropathy. *Neuromuscul Disord* 21:58–67.
49. Elks PM, et al. (2011) Activation of hypoxia-inducible factor-1α (Hif-1α) delays inflammation resolution by reducing neutrophil apoptosis and reverse migration in a zebrafish inflammation model. *Blood* 118:712–722.
50. Mitry RR (2009) Isolation of human hepatocytes. *Methods Mol Biol* 481:17–23.
51. Liaskou E, et al. (2011) Regulation of mucosal addressin cell adhesion molecule 1 expression in human and mice by vascular adhesion protein 1 amine oxidase activity. *Hepatology* 53:661–672.
52. Kaluz S, Kaluzová M, Stanbridge EJ (2008) Rational design of minimal hypoxia-inducible enhancers. *Biochem Biophys Res Commun* 370:613–618.
53. Facchinello N, et al. (2017) nr3c1 null mutant zebrafish are viable and reveal DNA-binding-independent activities of the glucocorticoid receptor. *Sci Rep* 7:4371.